LETTER

doi:10.1038/nature11265

Quantum phase transition in a resonant level coupled to interacting leads

Henok T. Mebrahtu[1], Ivan V. Borzenets[1], Dong E. Liu[1], Huaixiu Zheng[1], Yuriy V. Bomze[1], Alex I. Smirnov[2], Harold U. Baranger[1] & Gleb Finkelstein[1]

A Luttinger liquid is an interacting one-dimensional electronic system, quite distinct from the 'conventional' Fermi liquids formed by interacting electrons in two and three dimensions[1]. Some of the most striking properties of Luttinger liquids are revealed in the process of electron tunnelling. For example, as a function of the applied bias voltage or temperature, the tunnelling current exhibits a non-trivial power-law suppression[2,3]. (There is no such suppression in a conventional Fermi liquid.) Here, using a carbon nanotube connected to resistive leads, we create a system that emulates tunnelling in a Luttinger liquid, by controlling the interaction of the tunnelling electron with its environment. We further replace a single tunnelling barrier with a double-barrier, resonant-level structure and investigate resonant tunnelling between Luttinger liquids. At low temperatures, we observe perfect transparency of the resonant level embedded in the interacting environment, and the width of the resonance tends to zero. We argue that this behaviour results from many-body physics of interacting electrons, and signals the presence of a quantum phase transition[4,5]. Given that many parameters, including the interaction strength, can be precisely controlled in our samples, this is an attractive model system for studying quantum critical phenomena in general, with wide-reaching implications for understanding quantum phase transitions in more complex systems, such as cold atoms[6] and strongly correlated bulk materials[7].

Unlike two- and three-dimensional Fermi liquids, a Luttinger liquid completely 'dissolves' individual electrons, replacing them with collective plasmon waves. When, in the process of quantum-mechanical tunnelling, an external electron is added to the Luttinger liquid, the plasmons spread the charge through the system, akin to the ripples from a raindrop on the surface of a pond. At zero temperature, the tunnelling electron does not have the necessary energy to excite the plasmons. As a result, the tunnelling conductance between a normal metal and a Luttinger liquid, or between two Luttinger liquids, is suppressed at low temperature, with a power-law dependence on temperature[2,3].

Even more interesting is the case of resonant tunnelling, in which a single tunnel barrier between Luttinger liquids is replaced by a resonant level formed in a double-barrier quantum structure. Starting with the seminal work of ref. 8, this problem has received significant theoretical attention[9–12]. Perhaps the most spectacular prediction is the existence of resonance peaks with perfect conductance (full transparency), but vanishingly small width (infinite lifetime) at zero temperature[8]. These resonances require two Luttinger liquids that are symmetrically coupled to the resonant level. Several experiments have addressed resonant tunnelling in a Luttinger liquid in the low-temperature limit[2,13,14], but with no attempt to control the tunnelling strength. In this work, we create a system analogous to a Luttinger liquid by properly designing electron interactions in the resonant level's environment, and we tune the system to the symmetric coupling point.

We realize both the single-barrier tunnelling and the double-barrier resonant tunnelling regimes in short (~300-nm) segments of carbon nanotubes (Fig. 1a). Fig. 1b shows the representative electrical conductance through such a sample. The size quantization of electron states in the nanotube, combined with the mutual repulsion of the electrons, gives rise to a 'Coulomb blockade' pattern[15,16].

We first show Luttinger-liquid-like properties in tunnelling through a single barrier by tuning the gate voltage to Coulomb blockade valleys Y and Z of Fig. 1b, where no low-energy excitations exist in the nanotube. Electrons are then transmitted through the nanotube by co-tunnelling processes (see Supplementary Information section I). These processes are almost independent of energy, at scales smaller than the nanotube charging energy and level spacing (both millielectronvolts); at such energies, the nanotube should behave just like a single tunnel barrier.

The conductance in valleys Y and Z, plotted against bias voltage, V, shows a surprising zero-bias anomaly (ZBA), which gets progressively

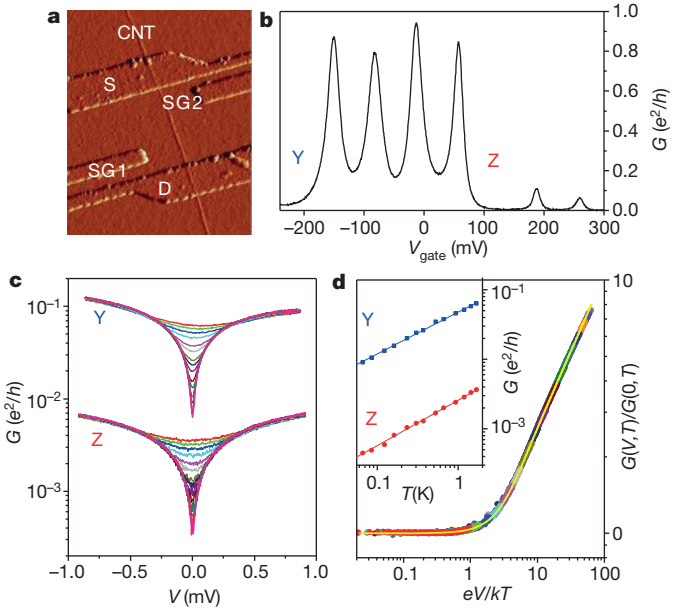

Figure 1 | Emulating Luttinger liquid with resistive environment. **a**, AFM image of the sample. The carbon nanotube (CNT) is contacted by two metal leads (S and D), forming a quantum dot. Two side gates (SG_1 and SG_2) control the coupling of the dot to the two leads, as used to obtain results shown in Fig. 2. **b**, Differential conductance $G \equiv dI/dV$ of a similar sample, as a function of the (back-)gate voltage, V_{gate}, at $T = 1.8$ K. We focus on Coulomb blockade valleys Y and Z, in which electron transport is conducted through co-tunnelling processes. **c**, Differential conductance versus bias voltage V, showing a pronounced zero-bias anomaly in both valleys. $T = 1.7$–0.03 K (top to bottom). **d**, $G(V,T)$ data measured in valley Y at different temperatures (coloured points) can be rescaled to collapse on the same universal curve, described by the theoretical expression of ref. 21 (yellow line). Inset shows the clear power-law dependence of zero-bias conductance $G(0,T)$ on temperature, with the same exponent in both valleys.

[1]Department of Physics, Duke University, Durham, North Carolina 27708, USA. [2]Department of Chemistry, North Carolina State University, Raleigh, North Carolina 27695, USA.

deeper as the temperature decreases (Fig. 1c). As the shape of the ZBA in the two valleys is the same up to an overall scale factor, the existence of the ZBA is not due to the nanotube itself. Indeed, the distinct feature of our samples is the metal leads to the nanotube, which are made rather resistive (kilohms; see Supplementary Information section II). 'Tunnelling with dissipation'[17] between such resistive leads is known to result in suppressed conductance: $dI/dV \equiv G \propto \max(k_B T, eV)^{2r}$ (refs 18–21), where I is current, G is conductance, k_B is the Boltzmann constant, T is temperature and $r = e^2R/h$, the ratio of the resistance of the leads, R, to the quantum resistance h/e^2. This expression is similar to the power-law suppression expected for tunnelling in a Luttinger liquid[2,3]. However, no real Luttinger liquid is present in our nanotube; at our operating temperatures, the length of an ideal clean nanotube would have to be about 100 μm to suppress the size quantization. Note the highly unusual appearance of the resistance in the exponent, which allows us to control the strength of tunnelling suppression simply by changing R.

Experimentally, the zero-bias conductance scales as $G(0,T) \propto T^{2r}$, with the same exponent $2r \approx 0.6$ found in both valleys (Fig. 1d inset); this value is consistent with the leads resistance ($R \approx 6.5\,k\Omega$ in this sample; see Supplementary Information section II). Furthermore, we can rescale the whole set of $G(V,T)$ curves measured in valley Y as shown in Fig. 1d, which presents $G(V,T)/G(0,T)$ as a function of eV/k_BT —a dimensionless ratio of bias to temperature. The yellow curve overlying the symbols is the result of the full theoretical expression describing tunnelling with dissipation[21], in which we use the same value of $r = 0.3$ extracted from the temperature dependence.

The expression used to fit the data in Fig. 1d is similar to the one describing tunnelling between two Luttinger liquids[22]. The similarity may be understood qualitatively: for both tunnelling in a dissipative environment and in a Luttinger liquid, the tunnelling electron's charge couples to a continuum of bosonic modes (plasmons); at zero energy (temperature or bias), the electron cannot excite the modes, and tunnelling is suppressed. Furthermore, the formal mapping of the two problems has been demonstrated for the single-barrier case in ref. 23. The recipe is to replace the Luttinger interaction parameter g by $1/(r + 1)$: *for example*, the case of vanishing dissipation, $r = 0$, corresponds to the non-interacting Luttinger liquid, $g = 1$. It is important to realize that for $r \neq 0$ electrons do in fact interact with each other through their coupling to the bosonic modes. We use the analogy between tunnelling in a dissipative environment and tunnelling in a Luttinger liquid through the rest of this text.

Having established Luttinger-liquid-like behaviour in single-barrier tunnelling, we now turn to the main focus of this work: resonant tunnelling between interacting leads. We study single-electron conductance peaks, similar to those shown in Fig. 1b, but measured on a different sample. A key feature of our experiment is the use of additional side gates to tune the coupling of the resonant level to the leads (Fig. 1a). Figure 2a shows the differential conductance map as a function of the side- and back-gate voltages. Clearly, the heights of the peaks change along the traces. For several of the peaks, the conductance reaches a maximum at some intermediate value of the side-gate voltage, indicating that the tunnelling rates from the resonant level to the source and the drain are equal: $\Gamma_S = \Gamma_D$ ('symmetric coupling').

We focus on peak X of Fig. 2a, with the side gate tuned so that the tunnelling is either symmetric (Fig. 2b) or asymmetric (Fig. 2c). Clearly, the two cases behave in markedly different ways. In the asymmetric case, the peak height decreases at low temperatures, while the width saturates[24]. In the symmetric case, the peak width decreases, while the peak height grows and reaches e^2/h. It is remarkable that the resonant tunnelling conductance can reach the unitary limit despite coupling to the interacting leads, which suppress tunnelling in the single-barrier case.

To account for the observed behaviour, we have developed a model (see Supplementary Information sections IV–VI) of a resonant level connected to two electron reservoirs, with excitation of environmental

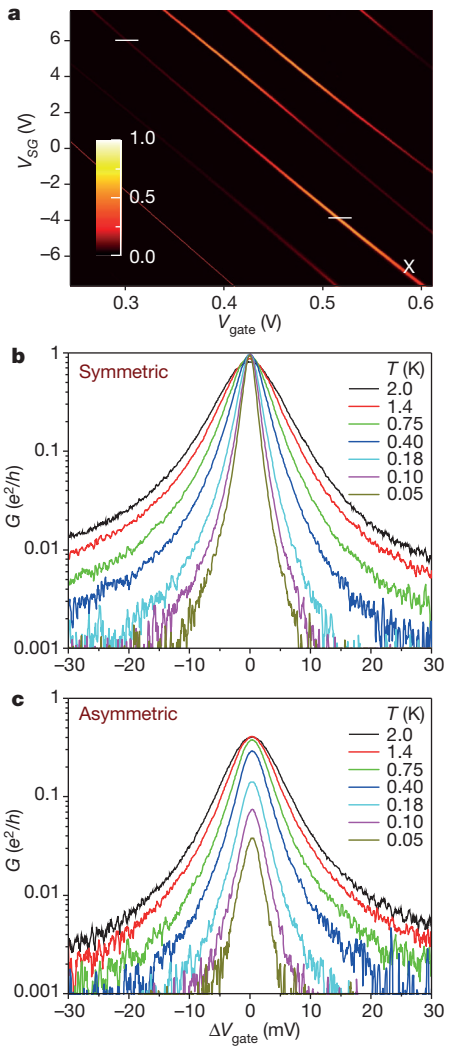

Figure 2 | Resonant lineshape: symmetric and asymmetric cases. **a**, Zero-bias differential conductance as a function of V_{gate} and the voltage V_{SG} applied to one of the side gates. Several peaks reach a maximal conductance of e^2/h (1.0 on colour scale) along their traces in the range shown here. The base temperature is $T = 50$ mK; a perpendicular magnetic field of 6 T is applied to select a single spin species. White horizontal lines and 'X' are explained below. **b**, **c**, Resonant conductance for symmetric (**b**) and asymmetric (**c**) coupling, measured at several temperatures on the peak marked 'X' in **a**, as a function of ΔV_{gate}, the gate voltage relative to the centre of the peak. The side-gate voltages are fixed at the values indicated by white lines in **a**. As the temperature is reduced, in the symmetric case the peak becomes taller and narrower. By contrast, in the asymmetric case, the peak becomes shorter and its width saturates.

modes represented by a dynamical phase associated with the tunnelling matrix element[18]. We show that the analogy between tunnelling with dissipation and tunnelling in a Luttinger liquid[22,23,25,26] further extends to our case of resonant tunnelling. Based on our mapping and the Luttinger-liquid predictions[8–12], in the case of symmetric coupling we expect the peak height to saturate at e^2/h (spinless case), and the resonance width to scale at low temperatures as $T^{r/(r+1)}$ (ref. 8). For asymmetric coupling, the resonance width is predicted to saturate at sufficiently low temperature[10,11], while the peak height should scale to zero as $G \propto T^{2r}$, featuring the same exponent as in the single-barrier (non-resonant) tunnelling.

Our experiment clearly corroborates these predictions (Fig. 3). Quantitatively, we extract $r \approx 0.75$ from the scaling of the asymmetric peak height, which agrees with the leads resistance in this sample. The width of the symmetric peak scales with an exponent of 0.45, consistent with $r/(r + 1) \approx 0.43$. (We discuss the accuracy of extracting the

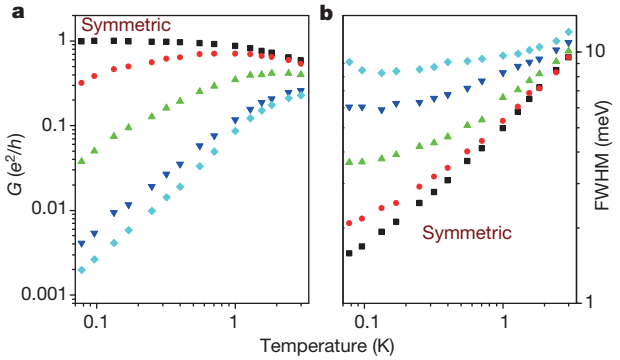

Figure 3 | Resonant peak parameters at different degrees of asymmetry. Conductance peak height (**a**) and width (**b**) measured at several values of V_{SG}, which controls the degree of asymmetry of the tunnel barrier. (Same sample as in Fig. 2, but different peak; from symmetric to most asymmetric, (V_{SG},V_{gate}) values range from (3.25,−0.518) to (−6.10,−0.692).) Note that in the symmetric case, with decreasing temperature, the peak height saturates at e^2/h, and its width (full width at half-maximum) monotonically decreases. In the asymmetric cases, the behaviour is the opposite: the width of the peak saturates, while the peak height decreases.

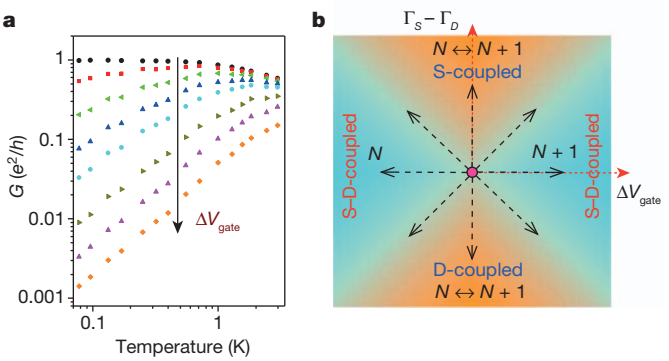

Figure 4 | Phase diagram and the quantum critical point. a, Conductance in the symmetric-coupling case, plotted versus temperature at different values of gate voltage. $\Delta V_{gate} = 0$, 0.7, 1.3, 2, 2.6, 5.0, 3.8 and 6.5 mV, from top to bottom. Note the similarity to Fig. 3a. **b**, Proposed phase diagram: the quantum critical point at the centre (symmetric coupling and $\Delta V_{gate} = 0$) has unitary conductance. Any deviations from this point result in vanishing conductance at $T = 0$.

exponents in Supplementary Information section III.) Overall, application of refs 8–12 to our experiment describes the observed behaviour remarkably well, in both the symmetric and asymmetric cases.

Note that the width of the conductance peak in the symmetric case decreases monotonically with decreasing temperature. In the limit of zero temperature, we expect that the conductance will equal zero everywhere, except for a singular point at the centre of the peak. When tunnelling asymmetry is introduced, the singular point disappears, and the low-temperature conductance tends to zero at any gate voltage, V_{gate}. This behaviour indicates a QPT for symmetric coupling, $\Gamma_S = \Gamma_D$. Technically, we refer to a 'boundary' QPT, in which only a local part of a larger system (local site plus environment) undergoes the transition (see, for example, ref. 5). QPTs found in strongly correlated bulk materials are often explained by invoking interactions between local sites and collective modes[4]. In the same spirit, our observation provides an example of a QPT in a highly tunable system that emulates such a 'local site' (that is, the resonant level), embedded in an interacting host.

Following ref. 12, we map our model in the $r = 1$ case onto the exotic two-channel Kondo model[27,28], for which a QPT is known to occur exactly for symmetric coupling[9]. (See Supplementary Information section V for details.) In both models, the origin of the quantum critical behaviour is the competition between the two channels attempting to screen the local site (spin or resonant level).

Intermediate values of r, between 0 and 1, do not allow for a simple interpretation in terms of any Kondo model with non-interacting leads, but represent a continuous evolution between the non-interacting resonant level at $r = 0$ and the two-channel Kondo model[9,29]. The critical exponents describing the system parameters close to the quantum critical point are not fixed, but are controlled by the value of r. Thus, our system not only provides new insight into the two-channel Kondo model—a model example of quantum criticality—but also gives access to a new family of quantum critical points for $r > 0$.

The QPT observed here is different from the various QPTs observed[30] and predicted[25] in quantum dots coupled to a single screening channel; indeed, there the QPTs are of the Kosterlitz–Thouless type, whereas in our case the QPT is of second order (see Supplementary Information section VI). Furthermore, in our case, the key ingredient that enables the QPT is the symmetric coupling to the two leads, which allows for their competition; the interaction in the leads (finite r) prevents their hybridization.

Finally, the conductance in the symmetric case can be plotted as a function of temperature for several values of ΔV_{gate} (Fig. 4a). The similarity with Fig. 3a is striking; apparently, one can tune away from the unitary resonance either by inducing asymmetry (Fig. 3a) or by applying the gate voltage (Fig. 4a)[8], with virtually the same results. Note that the downturn of peak height in Figs 3a and 4a occurs at progressively lower temperature as either the degree of asymmetry or ΔV_{gate} is reduced. Clearly, a new energy scale is emerging in the system, controlled by proximity to the quantum critical point[8,10,11]. We anticipate that this scale should vanish exactly at that point. We therefore propose the phase diagram shown in Fig. 4b, with a quantum critical point at $\Gamma_S = \Gamma_D$, $\Delta V_{gate} = 0$ (I. Affleck, personal communication). The four quadrants represent the states of the nanotube filled with N or $N + 1$ electrons, or coupled more strongly to either the source or the drain. The boundaries between the quadrants are smeared, and at $T = 0$ the conductance tends to zero everywhere, except at the quantum critical point.

In conclusion, we have investigated resonant tunnelling between interacting leads emulating Luttinger liquids. For symmetric coupling of the spinless resonant level to the two leads, and on resonance, the low-temperature conductance saturates at the unitary value of e^2/h. We associate this behaviour with a quantum critical point, which exists at $\Gamma_S = \Gamma_D$ in the presence of a finite interaction strength $r > 0$. Moving away from this point by inducing tunnelling asymmetry results in suppression of conductance at low temperature and smearing of the QPT. We believe that our work is the first example of a QPT in a highly tunable system, in which many parameters can be controlled, including the strength of interactions.

Received 13 April; accepted 24 May 2012.

1. Giamarchi, T. *Quantum Physics in One Dimension* (Oxford Univ. Press, 2004).
2. Chang, A. Chiral Luttinger liquids at the fractional quantum Hall edge. *Rev. Mod. Phys.* **75,** 1449–1505 (2003).
3. Deshpande, V. V., Bockrath, M. W., Glazman, L. I. & Yacoby, A. Electron liquids and solids in one dimension. *Nature* **464,** 209–216 (2010).
4. Sachdev, S. *Quantum Phase Transitions* 2nd edn (Cambridge Univ. Press, 2011).
5. Vojta, M. Impurity quantum phase transitions. *Phil. Mag.* **86,** 1807–1846 (2006).
6. Bloch, I. Ultracold quantum gases in optical lattices. *Nature Phys.* **1,** 23–30 (2005).
7. Si, Q. & Steglich, F. Heavy fermions and quantum phase transitions. *Science* **329,** 1161–1166 (2010).
8. Kane, C. L. & Fisher, M. P. A. Transmission through barriers and resonant tunnelling in an interacting one-dimensional electron gas. *Phys. Rev. B* **46,** 15233–15262 (1992).
9. Eggert, S. & Affleck, I. Magnetic impurities in half-integer-spin Heisenberg antiferromagnetic chains. *Phys. Rev. B* **46,** 10866–10883 (1992).
10. Nazarov, YuV & Glazman, L. I. Resonant tunnelling of interacting electrons in a one-dimensional wire. *Phys. Rev. Lett.* **91,** 126804 (2003).
11. Polyakov, D. G. & Gornyi, I. V. Transport of interacting electrons through a double barrier in quantum wires. *Phys. Rev. B* **68,** 035421 (2003).
12. Komnik, A. & Gogolin, A. O. Resonant tunnelling between Luttinger liquids: a solvable case. *Phys. Rev. Lett.* **90,** 246403 (2003).

13. Milliken, F., Umbach, C. & Webb, R. Indications of a Luttinger liquid in the fractional quantum Hall regime. *Solid State Commun.* **97,** 309–313 (1996).
14. Maasilta, I. & Goldman, V. Line shape of resonant tunnelling between fractional quantum Hall edges. *Phys. Rev. B* **55,** 4081–4084 (1997).
15. Kastner, M. A. Artificial atoms. *Phys. Today* **46,** 24–31 (1993).
16. Kouwenhoven, L. P. *et al.* in *Mesoscopic Electron Transport* (eds Sohn, L. L., Kouwenhoven, L. P. & Schön, G.) 105–214 (Kluwer, 1997).
17. Leggett, A. J. *et al.* Dynamics of the dissipative two-state system. *Rev. Mod. Phys.* **59,** 1–85 (1987).
18. Ingold, G.-L. & Nazarov, Y. V. in *Single Charge Tunnelling: Coulomb Blockade Phenomena in Nanostructures* (eds Grabert, H. & Devoret, M. H.) 21–107 (Plenum Press, 1992).
19. Flensberg, K., Girvin, S., Jonson, M., Penn, D. R. & Stiles, M. D. Quantum mechanics of the electromagnetic environment in the single-junction Coulomb blockade. *Physica Scripta* T42**,** 189–206 (1992). ≈.
20. Joyez, P., Esteve, D. & Devoret, M. H. How is the Coulomb blockade suppressed in high- conductance tunnel junctions? *Phys. Rev. Lett.* **80,** 1956–1959 (1998).
21. Zheng, W., Friedman, J., Averin, D. V., Han, S. & Lukens, J. E. Observation of strong Coulomb blockade in resistively isolated tunnel junctions. *Solid State Commun.* **108,** 839–843 (1998).
22. Sassetti, M., Napoli, F. & Weiss, U. Coherent transport of charge through a double barrier in a Luttinger liquid. *Phys. Rev. B* **52,** 11213–11224 (1995).
23. Safi, I&. Saleur, H. One-channel conductor in an ohmic environment: mapping to a Tomonaga-Luttinger liquid and full counting statistics. *Phys. Rev. Lett.* **93,** 126602 (2004).
24. Bomze, Y., Mebrahtu, H., Borzenets, I., Makarovski, A. & Finkelstein, G. Resonant tunnelling in a dissipative environment. *Phys. Rev. B* **79,** 241402(R) (2009).
25. Le Hur, K. & Li, M.-R. Unification of electromagnetic noise and Luttinger liquid via a quantum dot. *Phys. Rev. B* **72,** 073305 (2005).
26. Florens, S., Simon, P., Andergassen, S. & Feinberg, D. Interplay of electromagnetic noise and Kondo effect in quantum dots. *Phys. Rev. B* **75,** 155321 (2007).
27. Hewson, A. *The Kondo Problem to Heavy Fermions* (Cambridge Univ. Press, 1997).
28. Potok, R. M., Rau, I. G., Shtrikman, H., Oreg, Y. & Goldhaber-Gordon, D. J. Observation of the two-channel Kondo effect. *Nature* **446,** 167–171 (2007).
29. Goldstein, M. & Berkovits, R. Capacitance of a resonant level coupled to Luttinger liquids. *Phys. Rev. B* **82,** 161307 (2010).
30. Roch, N., Florens, S., Bouchiat, V., Wernsdorfer, W. & Balestro, F. Quantum phase transition in a single-molecule quantum dot. *Nature* **453,** 633–637 (2008).

Supplementary Information is linked to the online version of the paper at www.nature.com/nature.

Acknowledgements We appreciate discussions with I. Affleck, D. V. Averin, A. M. Chang, C. H. Chung, S. Florens, M. Goldstein, L. I. Glazman, K. Ingersent, K. Le Hur, M. Lavagna, A. H. MacDonald, Yu. V. Nazarov, D. G. Polyakov and M. Vojta. We thank J. Liu for providing the nanotube growth facilities and W. Zhou for helping to optimize the nanotube synthesis. The work was supported by US DOE awards DE-SC0002765, DE-SC0005237 and DE-FG02-02ER15354.

Author Contributions H.T.M., I.V.B. and G.F. designed the experiment. H.T.M. fabricated the samples. H.T.M., I.V.B., Y.V.B., A.S. and G.F. conducted the experiment. H.T.M. and G.F. analysed the data. H.T.M, D.E.L., H.Z., H.U.B. and G.F. interpreted the data. D.E.L., H.Z. and H.U.B. developed the theory.

Author Information Reprints and permissions information is available at www.nature.com/reprints. The authors declare no competing financial interests. Readers are welcome to comment on the online version of this article at www.nature.com/nature. Correspondence and requests for materials should be addressed to G.F. (gleb@phy.duke.edu).